CHEMISTRY
A EUROPEAN JOURNAL

DOI: 10.1002/chem.200800344

Cobalt–Lanthanide Coordination Polymers Constructed with Metalloligands: A Ferromagnetic Coupled Quasi-1D Dy^{3+} Chain Showing Slow Relaxation

You-Gui Huang,[a] Xiu-Teng Wang,[b] Fei-Long Jiang,[a] Song Gao,*[b] Ming-Yan Wu,[a] Qiang Gao,[a] Wei Wei,[a] and Mao-Chun Hong*[a]

Abstract: Four types of cobalt–lanthanide heterometallic compounds based on metalloligand $Co(2,5\text{-pydc})_3^{3-}$ (2,5-H_2pydc = pyridine-2,5-dicarboxylate acid), $[Ln_2Co_2(2,5\text{-pydc})_6(H_2O)_4]_n \cdot 2n\,H_2O$ (**1**) (Ln = Tb, Dy for **1a**, **1b** respectively), $[Tb_2Co_2(2,5\text{-pydc})_6(H_2O)_4]_n \cdot 3n\,H_2O$ (**2**), $[Tb_2Co_2(2,5\text{-pydc})_6(H_2O)_9]_n \cdot 4n\,H_2O$ (**3**), and $[LaCo(2,5\text{-pydc})_3(H_2O)_2]_n \cdot 2n\,H_2O$ (**4**) have been synthesized. Compound **1** has a layer structure with well-isolated carboxylate-bridged Ln^{3+} chains, compound **2** is a three-dimensional (3D) porous network with Tb^{3+} chains that are also well isolated and carboxylate bridged, **3** is a layer structure based on dinuclear units, and **4** is a 3D network with boron nitride (BN) topology. DC magnetic studies reveal ferromagnetic coupling in all the carboxylate-bridged Ln^{3+} chains in **1a**, **1b**, and **2**. Compared to the silence of the out-of-phase ac susceptibility of **2**, above 1.9 K the magnetic relaxation behavior of both **1a** and **1b** is slow like that of a single-chain magnet.

Keywords: cobalt · coordination polymers · heterometallic complexes · lanthanides · magnetic properties

Introduction

Single-molecule magnets (SMMs) elicit intense interest as they represent a molecular (or bottom-up) approach to nanoscale magnetism.[1] They straddle the classical/quantum interface, exhibiting not just the classical property of magnetization hysteresis, but also the quantum properties of quantum tunneling of the magnetization (QTM),[2] and quantum phase interference.[3] They are also candidates for future devices for information storage and quantum computation. This field was further expanded by the discovery of the polymeric compound, $[Co(hfac)_2(NITPhOMe)]$ (hfac = hexafluoroacetylacetonate, NITPhOMe = 4′-methoxyphenyl-4,4,5,5-tetramethylimidazoline-1-oxyl-3-oxide), which displays slow relaxation and hysteresis behavior.[4] This slow magnetization dynamic was explained with Glauber's model for Ising spin chains.[4] Recently, much effort has gone into the synthesis of this kind of new compound, known as a single-chain magnet (SCM).[5–9] However, the rational design of SCMs has been hampered by the difficulty in combining the three strict requirements for the desired behavior, namely high Ising anisotropy of the magnetic centers, strong intrachain ferromagnetic interactions between the high-spin magnetic units, and weak interchain interactions.[10–11] There are two strategies in the search for new SCMs: to link SMM building blocks covalently in a rational manner to control the dimensions of the structure and magnitude of the inter-SMM magnetic interaction;[9a,11,12] and (more straightforwardly) to link paramagnetic centers appropriately into nanowires or structures with well-isolated nanowires that might provide the desired properties.[5–8,9b,13]

We have developed a new metalloligand, $[Co(2,5\text{-Hpydc})_3]\cdot 3\,H_2O$ (2,5-H_2pydc = pyridine-2,5-dicarboxylate acid) in which the Co^{3+} is octahedrally coordinated with three N and three O atoms from three 2,5-Hpydc moieties. The metalloligand $[Co(2,5\text{-pydc})_3]^{3-}$ (hereafter, $[Co(2,5\text{-pydc})_3]^{3-}$ is abbreviated as L) has two kinds of Lewis-base coordination groups: 2-carboxylate (group A) and 5-carboxylate (group B) moieties (Figure 1). Group A has weaker bridging capability than group B because of its weak elec-

[a] Dr. Y.-G. Huang, Prof. F.-L. Jiang, M.-Y. Wu, Q. Gao, W. Wei, M.-C. Hong
State Key Laboratory of Structural Chemistry
Fujian Institute of Research on the Structure of Matter
Fuzhou, Fujian 350002 (People's Republic of China)
Fax: (+86) 591-8371-4946
E-mail: hmc@fjirsm.ac.cn

[b] Dr. X.-T. Wang, Prof. S. Gao
College of Chemistry and Molecular Engineering
Peking University, Beijing 100871 (People's Republic of China)
Fax: (+86) 10-6275-1708
E-mail: gaosong@pku.edu.cn

Supporting information for this article, including experimental, structural, coordination, and physical details, is available on the WWW under http://dx.doi.org/10.1002/chem.200800344.

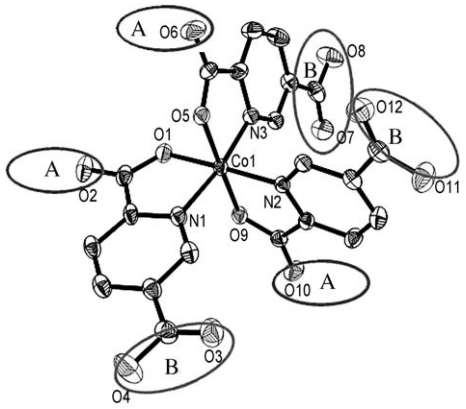

Figure 1. View of the metalloligand L ligand with two kinds of coordination group, A and B.

tron-donating and electrostatic power, and there is a considerable distance between adjacent groups B, enabling L to isolate magnetic nanowires well. In this regard, L may be a better candidate for SCMs than the original 2,5-H_2pydc if the choice of metal ions for coordination groups can be controlled. In this work, we used metalloligand L to link lanthanide ions covalently into the extended network, and obtained the cobalt–lanthanide heterometallic compounds $[Tb_2Co_2(2,5\text{-pydc})_6(H_2O)_4]_n\cdot 2n\,H_2O$ (**1a**), $[Dy_2Co_2(2,5\text{-pydc})_6(H_2O)_4]_n\cdot 2n\,H_2O$ (**1b**), $[Tb_2Co_2(2,5\text{-pydc})_6(H_2O)_4]_n\cdot 3n\,H_2O$ (**2**), $[Tb_2Co_2(2,5\text{-pydc})_6(H_2O)_9]_n\cdot 4n\,H_2O$ (**3**), and $[LaCo(2,5\text{-pydc})_3(H_2O)_2]_n\cdot 2n\,H_2O$ (**4**). Interestingly, simply by changing the cobalt resources used in the reaction system, we obtained entirely different compounds **1** (a layer with a well-isolated carboxylate-bridged Ln^{3+} chain) and **2** (a 3D porous framework with a well-isolated carboxylate-bridged Ln^{3+} chain). Additionaly, although the synthetic procedures for **1** and **4** are identical, their structures are completely different. This phenomenon may originate from lanthanide constriction. The static magnetic measurements on **1a**, **1b**, and **2** reveal ferromagnetic coupling in the carboxylate-bridged quasi-1D Ln^{3+} chains, and dynamic magnetic measurements show that **1a** and **1b** exhibit slow relaxation like SCM behavior. Therefore, this series of compounds provides a good system for comparative structural and magnetic studies.

Results and Discussion

Synthesis: Our synthesis of the metalloligand L under hydrothermal conditions was followed by reaction of L with $Tb(NO_3)_3\cdot 6H_2O$ to generate **1**. Alternatively we could obtain **1** in a one-step hydrothermal reaction of $Co(NO_3)_2\cdot 6H_2O$, $Tb(NO_3)_3\cdot 6H_2O$, and $H_2$2,5-pydc. However, by simply substituting $Co(Ac)_2\cdot 4H_2O$ (HAc = acetic acid) for the $Co(NO_3)_2\cdot 6H_2O$ in the system, we synthesized **2**, demonstrating that the anion influences the heterometallic framework. Each of three hydrothermal reactions can generate **4**: 1) L and $Ln(NO_3)_3\cdot 6H_2O$; 2) $Co(NO_3)_2\cdot 6H_2O$, $Ln(NO_3)_3\cdot 6H_2O$, and $H_2$2,5-pydc; 3) $Ln(NO_3)_3\cdot 6H_2O$, $Co(Ac)_2\cdot 4H_2O$ and $H_2$2,5-pydc. Furthermore, we also obtained the Sm, Eu, Gd, Ho, Er, Tm, and Yb analogues of **1**, the Dy analogue of **2** and the Pr and Nd analogues of **4**.

Structures: All of the asymmetric units in **1**, **2**, and **3** contain two eight-coordinated Ln^{3+} ions and two L metalloligands (Supporting Information, Figures S8–S10); the coordination modes of L^{A-G} in all the compounds are given in Figure S7 in the Supporting Information. In **1** and **2**, both Tb1 and Tb2 are surrounded by six carboxylate O atoms and two water molecules in a distorted trigonal dodecahedron. Each metalloligand L^A acts as a μ_4 bridge to link four Tb^{3+} ions in which the three 5-carboxylate groups from 2,5-pydc moieties adopt monodentate μ_2-η^1:η^1 bridging and μ_2-η^2:η^1 bridging modes, respectively, whereas each metalloligand L^B acts as a μ_5 bridge in which two O atoms of one 5-carboxylate group chelate a Tb^{3+} ion and the other two 5-carboxylate groups adopt μ_2-η^1:η^1 bridging modes. The Tb^{3+} ions are firstly bridged by two μ-carboxylate groups and a μ-carboxylate O atom into a dimer with an intradimer $Tb^{3+}\cdots Tb^{3+}$ distance of 4.485 Å. Interestingly, adjacent dimers are bridged by a μ-carboxylate group (interdimer $Tb^{3+}\cdots Tb^{3+}$ distance 5.992 Å) to form a chain (Figure 2a). Adjacent chains are further interlinked in layers by metalloligand L ligands with a shortest $Tb^{3+}\cdots Tb^{3+}$ distance of 13.065 Å (Figure 2b). Such layers are stacked along the *c* axis with lattice water molecules located between them (Supporting Information, Figure S12c). Tb^{3+} ions are linked through a Co^{3+} ion and two 2,5-pydc moieties of L^A to generate left-handed helical chains and also through those of L^B to form right-handed helical chains (Supporting Information, Figures S12a,b). The left- and right- handed helical chains are further interwoven by shared Tb^{3+} ions, giving rise to helical tubes with opposite chirality arranged alternately along the *a* axis (Fig-

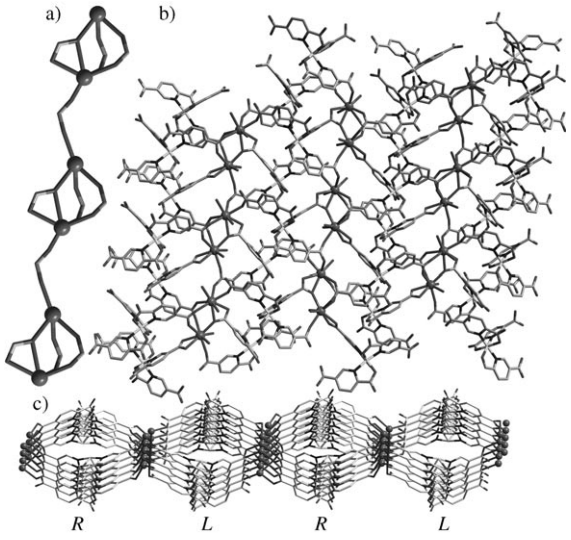

Figure 2. a) The carboxylate-bridged Tb^{3+} chain in **1a**. b) The layer structure of **1a** containing carboxylate-bridged Tb^{3+} chains. c) Helical tubes with opposite chirality in **1a**.

ure 2c). The remaining 2,5-pydc moieties ligate to Tb^{3+} ions and fill the tubes.

In **2**, the metalloligands L^C and L^D are in the same coordination mode as L^B in **1**. L^C ligands bridge the Tb^{3+} ions forming a layer based upon linear carboxylate-bridged $[Tb^{3+}]_4$ units. The $Tb^{3+}\cdots Tb^{3+}$ distances in the $[Tb^{3+}]_4$ unit are 5.160, 5.155, and 5.160 Å, respectively, and the $Tb^{3+}\cdots Tb^{3+}$ distance between the $[Tb^{3+}]_4$ units is 5.320 Å (Supporting Information, Figure S13b). However, L^D ligands bridge the Tb^{3+} ions forming a tape based on linear carboxyl-bridged $[Tb^{3+}]_4$ units (Supporting Information, Figure S13a). The tapes interlink with the layers described above by sharing Tb^{3+} ions to generate a porous three-dimensional network (Figure 3b) containing $[Tb^{3+}]_4$ units bridged by carboxylate

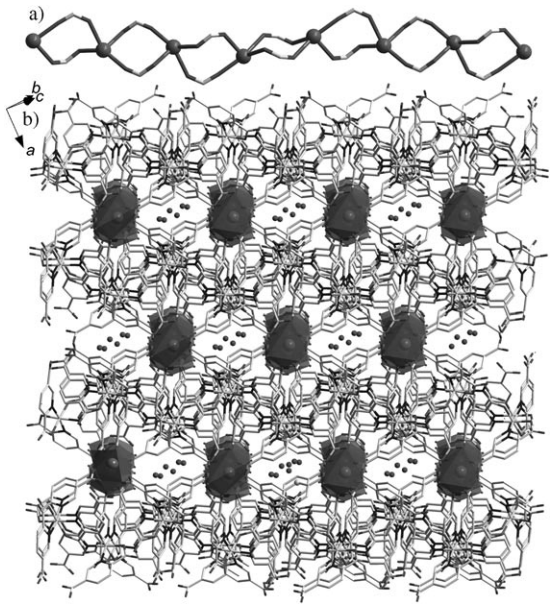

Figure 3. a) The carboxyl-bridged Tb^{3+} chain in **2**. b) The 3D porous network of **2** containing carboxyl-bridged Tb^{3+} chains.

to form a nanowire (Figure 3a). In the 3D network, each carboxylate-bridged Tb^{3+} chain connects with four others with an interchain $Tb^{3+}\cdots Tb^{3+}$ distance of about 13 Å. Interestingly, 1D lattice water-filled channels exist along the carboxylate-bridged Tb^{3+} chain.

In **3**, Tb1 is coordinated by three carboxylate O atoms and five water molecules while Tb2 is coordinated by four carboxylate O atoms and four water molecules. Each metalloligand L^E acts as a μ_2 bridge in which one 5-carboxylate group is free and the other two 5-carboxylate groups adopt a monodentate coordination mode; each metalloligand L^F acts as a μ_4 bridge in which two oxygen atoms of one 5-carboxylate group chelate a Tb^{3+} ion, one 5-carboxylate group adopts a monodentate coordination mode, and one 5-carboxylate group adopts aμ_2-η^1:η^1 bridging mode. The Tb^{3+} ions are firstly linked together by L^E to generate a chain formed by two kinds of dimers with an interdimer $Tb^{3+}\cdots Tb^{3+}$ distance of 12.817 Å (Figure 4a), arranged alternately. One kind of dimer is carboxylate bridged and the other is bridged by two 2,5-pydc moieties from L^E with intradimer $Tb^{3+}\cdots Tb^{3+}$ distances of 4.959 and 9.636 Å, respectively. The chains are further interlinked by L^F to form layers with shortest interchain $Tb^{3+}\cdots Tb^{3+}$ distance 7.470 Å (Figure 4b). As in **1**, such layers are stacked along the *a* axis with lattice water molecules located between them (Supporting Information, Figure S14).

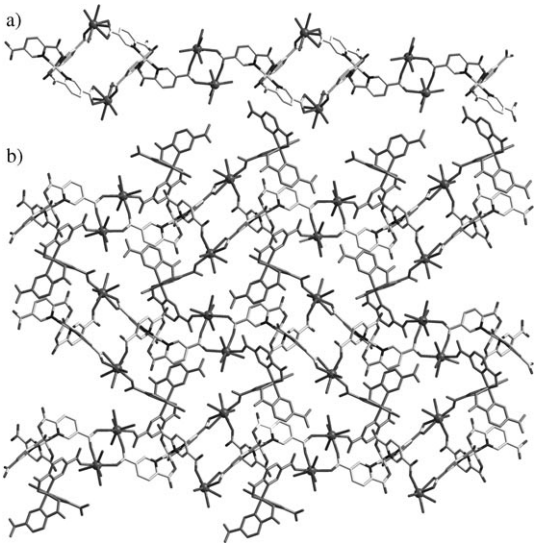

Figure 4. a) The chain based on two kinds of dimers in **3**. b) The layer structure formed by L^E linked chains in **3**.

In **4**, the asymmetric unit contains a nine-coordinated La^{3+} ion and a metalloligand L (Supporting Information, Figure S11). The La^{3+} ion is coordinated by seven carboxylate O atoms and two water molecules in a tricapped trigonal prism. Each metalloligand L^G acts as a μ_5 bridge with two 2-carboxylate groups ligated to two La^{3+} ions, one 5-carboxylate group adopting a monodentate coordination mode and the other two chelate coordination modes. The La^{3+} ions are interconnected through metalloligands L to generate an intricate 3D architecture. Herein, we describe it stepwise. Firstly, the La^{3+} ions are bridged through one 2,5-pydc moiety of L^G to form a chain (Figure 5a). Then, the remaining two 2,5-pydc moieties and the Co^{3+} ion of L^G connect the La^{3+} ions, forming a layer with (4×8^2) topology (Figure 5b). The layers interlink with the chains described above to generate the intricate structure (Figure 5c). In the network, each La^{3+} ion is linked to five L ligands and each L ligand is ligated to five La^{3+} ions, both thus defining five-connected nodes. From the topological viewpoint, the structure of **4** is a uninodal five-connected net with boron nitride (BN) topology and a $(4^3\times5\times6^5\times8)$ Schäfli symbol (Supporting Information, Figure S15).

Magnetic properties: Temperature-dependent magnetic susceptibility measurements for compounds **1a, 1b**, **2**, and **3** were performed on the polycrystalline samples in the 2–

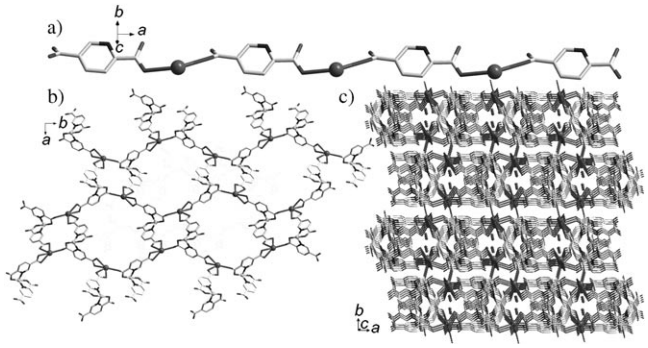

Figure 5. a) The chain formed by one 2,5-pydc moiety of L^G-bridged La^{3+} ions in **4**. b) The layer structure with (4×8^2) topology in **4**. c) The whole 3D framework of **4** with a BN net.

300 K range under 1000 Oe external field (Figure 6). For **1a**, $\chi_m T$ per Tb^{3+} ion is 11.23 $cm^3 K mol^{-1}$ at room temperature, almost equal to the expected value of 11.76 $cm^3 K mol^{-1}$ for

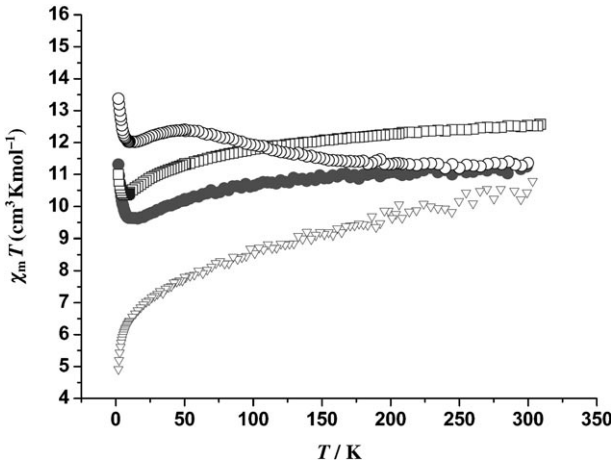

Figure 6. Temperature dependence of $\chi_m T$ for **1a**, **1b**, **2**, and **3** at 1000 Oe. **1a**:●, **1a**:□, **2**:○, **3**: ▽

a free Tb^{3+} ion with a $^7F_6$ ground state. As the temperature is lowered, $\chi_m T$ decreases to a minimum at about 16 K and then increases rapidly to reach 11.23 $cm^3 K mol^{-1}$ at 2 K. The decrease in $\chi_m T$ may be due to the depopulation of the Stark levels for a single Tb^{3+} ion,[14] and the increase at low temperature reveals dominant ferromagnetic interaction between Tb^{3+} ions in the carboxylate-bridged chain. For **1b**, $\chi_m T$ per Dy^{3+} ion at 300 K (12.54 cm^3 K mol^{-1}) is slightly lower than the expected value of 14.05 $cm^3 K mol^{-1}$ with a $^6H_{15/2}$ ground state. Similarly to **1a**, upon cooling, $\chi_m T$ decreases to a minimum and then increases rapidly to reach 11.00 $cm^3 K mol^{-1}$ at 2 K, showing dominant ferromagnetic coupling between Dy^{3+} ions in the carboxylate-bridged Dy^{3+} chain.

For **2**, $\chi_m T$ per Tb^{3+} ion is 11.89 $cm^3 K mol^{-1}$ and the χ_{mT} versus T plot is complicated. Upon cooling, $\chi_m T$ increases to a maximum at 50 K, then decreases to a minimum at about 14 K, and finally increases rapidly on further cooling, also demonstrating ferromagnetic coupling between Tb^{3+} ions in the carboxylate-bridged chain.

For **3**, $\chi_m T$ per Tb^{3+} ion is 10.81 $cm^3 K mol^{-1}$ and decreases continuously to 4.75 $cm^3 K mol^{-1}$ at 2 K. This continuous decrease may be due to the depopulation of the Stark levels for a single Tb^{3+} ion and/or to antiferromagntic interactions between Tb^{3+} ions within dinuclear units.[14] We also measured the magnetic susceptibility of the Sm, Eu, Gd, Ho, Er, Tm, and Yb analogues of **1** and the Dy analogue of **2**, but no clear ferromagnetic coupling was observed in any of these compounds (Supporting Information, Figures S19 and S20).

For the observed ferromagnetic coupling between Ln^{3+} ions in the carboxylate-bridged chains, we measured the field dependence of the magnetization (M) in the −8 to +8 T field range and the ac magnetic susceptibility for **1a**, **1b**, and **2**. The M–H curves for all three compounds are very similar. The fast saturated variations on the isothermal magnetization (M) versus the applied field (H) curve further confirm the dominant intrachain ferromagnetic coupling for the three compounds (Figure 7). The saturation values of 5.9 Nβ and 6.4 Nβ for **1a** and **2** are slower than that expected (9 Nβ for each Tb^{3+} ion). This is due to the crystal-field effect on the Tb^{3+} ions, which removes the 13-fold degeneracy of the $^7F_6$ ground state.[18a] The saturation value of 5.4 Nβ for **1b** is almost equal to that of other dysprosium compounds, assuming the crystal-field effect.[18e]

First, we measured the ac magnetic susceptibility for **1a**, **1b**, and **2** in zero applied dc field. The linear variation of $\ln(\chi'_m T)$ versus T^{-1} observed for all three compounds indicates a strong Ising-like chain (Supporting Information, Figure S16). The low-temperature deviation from the linear regime of **1b** is consistent with a geometrical limitation of the correlation length owing to the presence of defects.[15] No irreversibility was observed in the zero-field-cooled (ZFC) and field-cooled (FC) magnetization for any of the three compounds, thereby indicating no long-range order and further confirming their 1D nature (Supporting Information, Figure S17).[16] No clearly frequency-dependent out-of-phase signal was observed for **2** above 2 K, which excludes the possibility that **2** exhibits SCM behavior.[5–8,9b,13] However, a slightly frequency-dependent out-of-phase signal was observed for **1a**, and clearly frequency-dependent signals, both in-phase and out-of-phase, were observed for **1b** (Figure 8). This behavior is positive proof for the SCM, although it is not conclusive, since spin-glass or random-domain magnets can also lead to such signals.[17] To investigate this behavior further, the isothermal frequency-dependent ac susceptibility of **1b** was measured to evaluate the effective energy barrier and relaxation time (Figure 9). The data were fitted by a generalized Debye model (for details see Supporting Information, Table S7). The τ values obtained were fitted by the Arrhenius law $[\tau=\tau_0\exp(U_{eff}/k_BT)]$, giving $\alpha\approx0.18$, $U_{eff}=4.89$ K, $\tau_0=7.56\times10^{-8}$ s, and $R=2.35\times10^{-6}$, $R=\Sigma(\ln\sigma_{obs}-\ln\tau_{calc})^2/\Sigma\ln\tau$, indicating a narrow distribution of relaxation times (Figure 10). It is known that

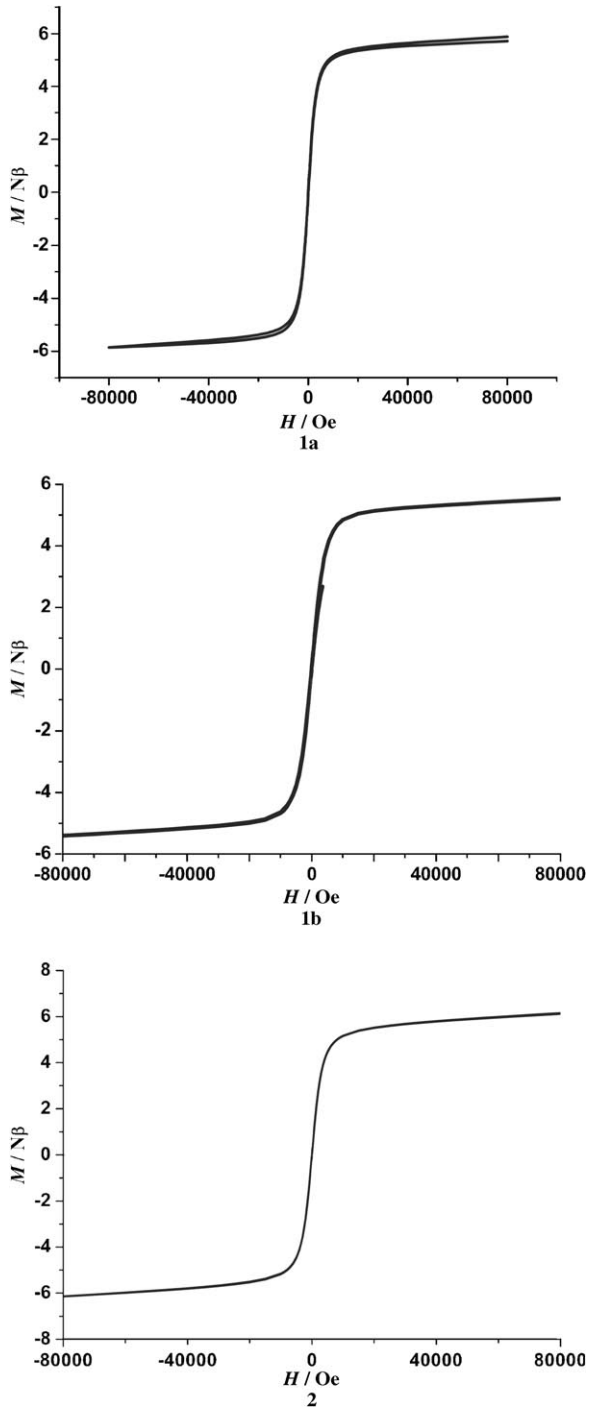

Figure 7. Plots of M versus H for **1a**, **1b**, and **2** at 2 K.

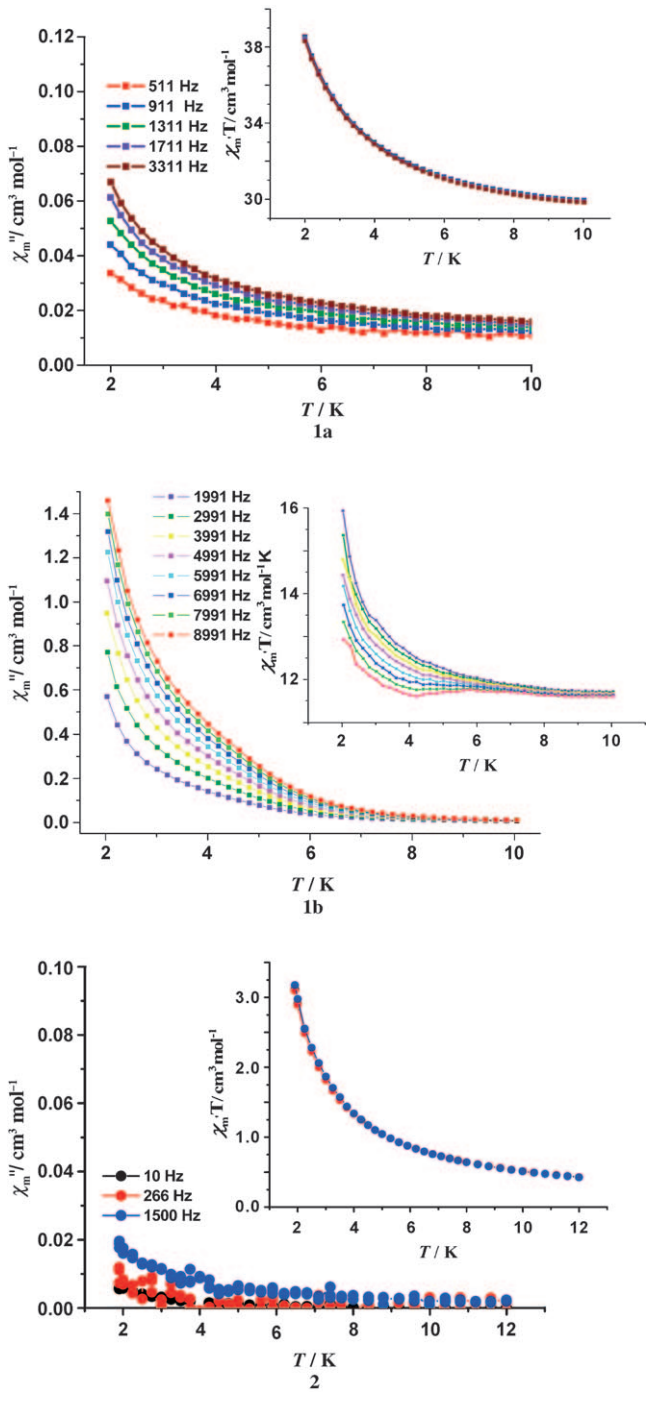

Figure 8. Temperature dependence of ac χ_m at different frequencies for **1a**, **1b**, and **2** ($H_{dc}=0$ Oe, $H_{ac}=3$ Oe).

an ideal SMM or SCM is likely to possess a single relaxation time ($\alpha=0$) whereas a spin glass would show a wide range of relaxation processes ($\alpha=\rightarrow1$). The α, U_{eff} and τ_0 values obtained allow us to confirm that we are not faced with a spin-glass behavior, and are comparable to those of some other SCMs or SMMs.[18]

It was noticed that the energy gap (U_{eff}), which is well known to be relevant to the relaxation time (τ_0) in an SCM, can be tuned by an applied field, so we recorded χ_{ac} versus applied dc fields at 2 K.[1c] As predicted, a strong field dependence of χ_{ac} was observed and the maximum of χ''_m occurred at $H=400$ Oe (Supporting Information, Figure S18). A dc field of 400 Oe was therefore selected to investigate the temperature dependence of the dynamic susceptibility. As a result, both in-phase and out-of-phase frequency-dependent signals are more visible, and the maxima of $\chi'_m T$ appeared (Figure 11).

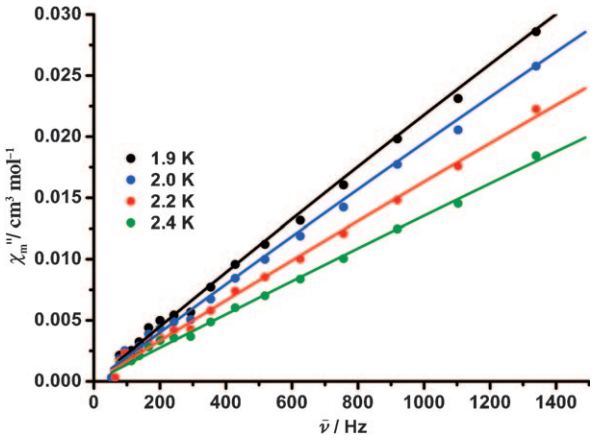

Figure 9. Frequency dependence of the imaginary parts (χ_m'') of the ac susceptibility for **1b**.

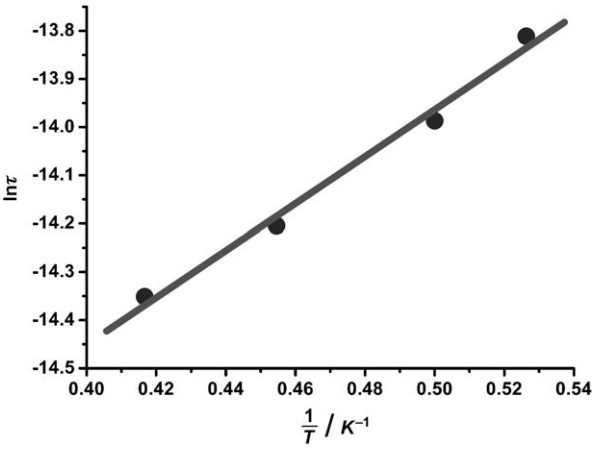

Figure 10. Plot of lnτ versus $1/T$ for **1b** deduced from the modes observed on the χ_m'' versus ν data.

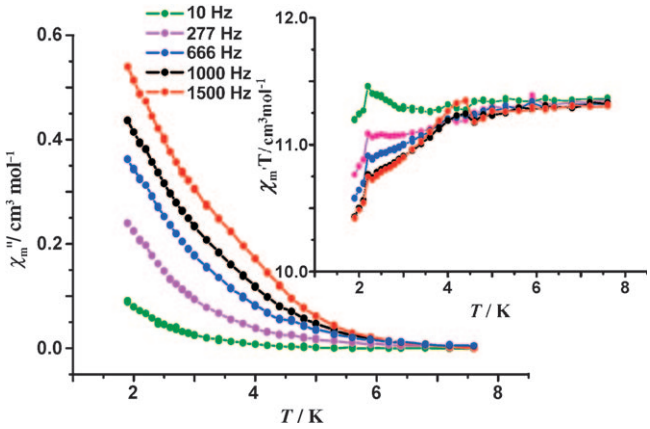

Figure 11. Temperature dependence of ac χ_m'' at different frequencies for **1b** (H_{dc} = 400 Oe, H_{ac} = 3 Oe).

Conclusion

We have demonstrated that both the cobalt source and lanthanide constriction influence the compositions and structures of the four lanthanide-cobalt coordination polymers based on metalloligand $Co(2,5\text{-pydc})_3^{3-}$ that were synthesized. Compounds **1a** and **1b** have a layer structure with well-isolated carboxylate-bridged Ln^{3+} chains, **2** is a 3D porous network with well-isolated carboxylate-bridged Tb^{3+} chains as well, **3** is a layer structure based on dinuclear units, and **4** is a 3D network with BN topology. The Ln^{3+} chains in **1a**, **1b**, and **2** cause them to tend to behave like single chain magnets (SCMs). Intrachain ferromagnetic coupling in **1a**, **1b** and **2** has been revealed by dc magnetic measurements, and dynamic magnetic measurements show that **1a** and **1b** exhibit slow relaxation resembling SCM behavior. The metalloligand L is expected to be a good candidate for constructing a new family of SCMs.

Experimental Section

Thermal analyses: Thermal gravimetric analysis was carried out for polycrystalline samples of metalloligand L and compounds **1a**–**4** in the range 30–800 °C (Supporting Information, Figure S6). For L, the first weight loss of 9.87 % in the range 30–180 °C corresponded to the loss of lattice water molecules (calcd 8.88 %). The complex began to decompose at 260 °C. For **1a**, the first weight loss of 7.37 % in the range 30–230 °C corresponded to the loss of lattice and coordinated water molecules (calcd 7.04 %). The network decomposed at 370 °C. For **1b**, the first weight loss of 8.07 % in the range 30–300 °C corresponded to the loss of lattice and coordinated water molecules (calcd 7.01 %) and the network decomposed at 360 °C. For **2**, the first weight loss of 9.19 % in the range 30–220 °C corresponded to the loss of lattice and coordinated water molecules (calcd 8.11 %). The network began to decompose at 280 °C. Compound **3**, with increasing temperature, began to decompose at 620 °C. For **4**, the first weight loss of 10.12 % in the range 30–150 °C corresponded to the loss of lattice and coordinated water molecules (calcd 9.41 %) and the network began to decompose at 260 °C.

Syntheses

Metalloligand L: A mixture of $Co(NO_3)_2{\cdot}6H_2O$ (0.058 g, 0.2 mmol) and 2,5-H_2pydc (0.096 g, 0.6 mmol) in H_2O (5 mL) was sealed in a 25 mL Teflon-lined bomb at 160 °C for 3 days, then cooled slowly at 5 °C h^{-1} to room temperature. Red prismatic crystals of L were recovered by filtration, washed with distilled water, and air-dried (0.094 g, 78 % based upon 2,5-H_2pydc). IR (KBr): $\tilde{\nu}$ = 3419(b), 1638(s), 1457(m), 1338(m), 810(w), 752(m), 696(m), 615(m), 523 cm^{-1} (w); elemental analysis calcd (%) for $C_{21}H_{15}CoN_3O_{15}$ (608.29): C 41.43, H 2.66, N 6.90; found: C 41.40, H 2.63, N 6.91.

*Compounds **1a** and **1b**: Method A*: As for metalloligand L, using a mixture of $Co(NO_3)_2{\cdot}6H_2O$ (0.058 g, 0.2 mmol), $Ln(NO_3)_3{\cdot}6H_2O$ (Ln = Tb, Dy for **1a**, **1b** respectively), and 2,5-H_2pydc (0.096 g, 0.6 mmol). Red prismatic crystals of **1a** and **1b** were recovered by filtration, washed with distilled water, and air-dried (0.121g, Yield: 79% for **1a**; 0.112g, Yield: 73% for **1b** based upon 2,5-H_2pydc). IR (KBr) for **1a**: $\tilde{\nu}$ = 3430(b), 1630(s), 1457(m), 1334(m), 816(w), 754(m), 698(m), 615(m), 520 cm^{-1} (w); IR (KBr) for **1b**: $\tilde{\nu}$ = 3432(b), 16330(s), 1458(m), 1339(m), 818(w), 751(m), 698(m), 614(m), 526 cm^{-1} (w); elemental analysis calcd (%) for $C_{42}H_{30}Co_2N_6O_{30}Tb_2$ (**1a**) (1534.42): C 32.85, H 2.09, N 5.47; found: C 32.815, H 2.06, N 5.43; elemental analysis calcd (%) for $C_{42}H_{30}Co_2NDy_{26}O_{30}$ (**1b**) (1541.58): C 32.69, H 1.95, N 5.45; found: C 32.65, H 1.98 N 5.43.

Table 1. Crystal data for metalloligand L and **1a**–**4**.

	Metalloligand	**1a**	**1b**	**2**	**3**	**4**
formula	$C_{21}H_{15}CoN_3O_{15}$	$C_{42}H_{30}Co_2N_6O_{30}Tb_2$	$C_{42}H_{30}Co_2Dy_2N_6O_{30}$	$C_{42}H_{34}Co_2N_6O_{31}Tb_2$	$C_{42}H_{46}Co_2N_6O_{38}Tb_2$	$C_{21}H_{17}CoLaN_3O_{16}$
M_r	608.29	1534.42	1541.58	1554.45	1678.55	765.22
crystal size [mm]	0.85×0.43×0.35	0.25×0.10×0.05	0.10×0.06×0.04	0.12×0.10×0.03	0.16×0.08×0.02	0.18×0.15×0.08
crystal system	triclinic	monoclinic	monoclinic	triclinic	monoclinic	monoclinic
space group	$P\bar{1}$	$P2_1/c$	$P2_1/c$	$P\bar{1}$	$P2_1/c$	$P2_1/c$
a [Å]	7.0885(6)	22.8717(14)	22.888(2)	12.639(4)	13.525(3)	11.8098(2)
b [Å]	13.4398(8)	10.2309(5)	10.2336(7)	14.490(5)	24.889(5)	21.74100(10)
c [Å]	13.5566(7)	21.2820(16)	21.276(2)	14.828(6)	18.843(4)	10.0143(2)
α [°]	75.481(11)			88.661(14)		
β [°]	84.382(13)	105.910(2)	106.053(6)	73.830(9)	109.908(4)	103.3680(10)
γ [°]	86.320(12)			71.340(11)		
V [Å^3]	1243.21(14)	4789.2(5)	4788.9(7)	2464.6(15)	5964(2)	2501.57(7)
Z	2	4	4	2	4	4
ρ_{calcd} [g cm^{-3}]	1.625	2.106 1	2.138	2.095	1.869	2.032
μ [mm^{-1}]	0.773	3.710	3.877	3.607	2.977	2.437
T [K]	293	293	293	293	293	293
$\lambda(Mo_{K\alpha})$ [Å]	0.71073	0.71073	0.71073	0.71073	0.71073	0.71073
reflections collected	9678	36862	36405	19286	47140	13282
unique reflections	5622	10970	10964	19312	13675	4749
observed reflections	4230	9534	8306	12779	11119	3638
parameters	361	739	739	744	796	379
GOF on F^2	1.036	1.082	1.125	1.038	1.071	1.113
R_1[a]	0.0834	0.0406	0.0793	0.0796	0.0656	0.0408
R_w[b]	0.2567	0.0955	0.1847	0.2685	0.2198	0.0815
max/min $\Delta\rho$ [e Å^{-3}]	1.889/−0.912	2.224/−1.247	2.980/−1.918	4.511/−4.181	2.517/−3.274	2.224/−1.247

[a] $R_1=\Sigma||F_o|-|F_c||/\Sigma|F_o|$. [b] $R_w=[\Sigma w(F_o^2-F_c^2)^2/\Sigma w(F_o^2)^2]^{1/2}$.

Method B: As for metalloligand L, using a mixture of [Co(2,5-Hpydc)$_3$]·3H$_2$O (0.121 g, 0.2 mmol) and Ln(NO$_3$)$_3$·6H$_2$O (Ln = Tb, Dy for **1a**, **1b,** respectively). Red prismatic crystals of **1a** and **1b** were recovered by filtration, washed with distilled water, and air-dried. Yield: 70% (0.108 g) for **1a**, 64% (0.099 g) for **1b** based on [Co(2,5-Hpydc)$_3$]·3H$_2$O.

Compound ***2***: As for metalloligand L, using a mixture of Co(Ac)$_2$·4H$_2$O (0.050 g, 0.2 mmol), Tb(NO$_3$)$_3$·6H$_2$O (0.091 g, 0.2 mmol), and 2,5-H$_2$pydc (0.096 g, 0.6 mmol). Red prismatic crystals of **1** were recovered by filtration, washed with distilled water, and air-dried. Yield: 74% (0.115 g) based on 2,5-H$_2$pydc; IR (KBr): $\tilde{\nu}$ = 3414(b), 1633(s), 1452(m), 1334(m), 816(w), 752(m), 690(m), 615(m), 523 cm^{-1} (w); elemental analysis calcd (%) for $C_{42}H_{34}Co_2N_6O_{31}Tb_2$ (**2**) (1554.45): C 32.42, H 2.19, N 5.40; found: C 32.45, H 2.16, N 5.38.

Compound ***3***: A mixture of Co(Ac)$_2$·4H$_2$O (0.050 g, 0.2 mmol), Tb(NO$_3$)$_3$·6H$_2$O (0.091 g, 0.2 mmol), and 2,5-H$_2$pydc (0.096 g, 0.6 mmol) in H$_2$O (5 mL) was sealed in a 25 mL Teflon-lined bomb at 160 °C for 3 days, then cooled slowly at 5 °C h^{-1} to room temperature. Red prismatic crystals of **2** were recovered by filtration, then the red solution was evaporated at room temperature without stirring. After several days red prismatic crystals of **3** were obtained and air-dried. Yield: 84% (0.143 g) based on 2,5-H$_2$pydc; IR (KBr): $\tilde{\nu}$ = 3418(b), 1636(s), 1457(m), 1339(m), 818(w), 752(m), 690(m), 619(m), 527 cm^{-1} (w); elemental analysis calcd (%) for $C_{42}H_{46}Co_2N_6O_{38}Tb_2$ (**3**) (1678.55): C 30.03, H 2.74, N 5.00; found: C 30.01, H 2.72, N 5.02.

Compound ***4***: *Method A*: As for metalloligand L, using a mixture of Co(NO$_3$)$_2$·6H$_2$O (0.058 g, 0.2 mmol), La(NO$_3$)$_3$·6H$_2$O (0.087 g, 0.2 mmol), and 2,5-H$_2$pydc (0.096 g, 0.6 mmol). Red prismatic crystals of **4** were recovered by filtration, washed with distilled water, and air-dried. Yield: 80% (0.123 g) based on 2,5-H$_2$pydc; IR (KBr): $\tilde{\nu}$ = 3442(b), 1633(s), 1462(m), 1324(m), 818(w), 756(m), 690(m), 616(m), 520 cm^{-1} (w); elemental analysis calcd (%) for $C_{21}H_{17}CoLaN_3O_{16}$ (**4**) (765.22): C 32.94, H 2.22, N 5.49; found: C 32.91, H 2.20, N 5.45.

Method B: As for metalloligand L, using a mixture of Co(Ac)$_2$·4H$_2$O (0.050 g, 0.2 mmol), La(NO$_3$)$_3$·6H$_2$O (0.087 g, 0.2 mmol), and 2,5-H$_2$pydc (0.096 g, 0.6 mmol). Red prismatic crystals of **4** were recovered by filtration, washed with distilled water, and air-dried. Yield: 74% (0.114 g) based on 2,5-H$_2$pydc.

Method C: As for metalloligand L, using a mixture of [Co(2,5-Hpydc)$_3$]·3H$_2$O (0.121 g, 0.2 mmol), La(NO$_3$)$_3$·6H$_2$O (0.087 g, 0.2 mmol), and 2,5-H$_2$pydc (0.096 g, 0.6 mmol). Red prismatic crystals of **4** were recovered by filtration, washed with distilled water, and air-dried. Yield: 86% (0.131 g) based on [Co(2,5-Hpydc)$_3$]·3H$_2$O).

Structures: Crystal data for **1**–**4** are summarized in Table 1. For all the compounds, the positions of the diffraction peaks of the experimental and simulated XRD patterns corresponded well (Supporting Information, Figures S1–S5), thus indicating phase purity of the as-synthesized samples. Other phase-purity lanthanide–cobalt coordination polymers such as [Ln$_2$Co$_2$(2,5-pydc)$_6$(H$_2$O)$_4$]$_n$·2nH$_2$O (Ln = Sm , Eu, Gd, Ho, Er, Tm, Yb) analogous to **1**, and [LnCo(2,5-pydc)$_3$(H$_2$O)$_2$]$_n$·2nH$_2$O (Ln = Pr, Nd) analogous to **4** were obtained. CCDC-673969 (metalloligand L), 673970 (**1a**), 673971 (**1b**), 673972 (**2**), 673973 (**3**), and 673974 (**4**) contain the supplementary crystallographic data for this paper. These data can be obtained free of charge from the Cambridge Crystallographic Data Center via www.ccdc.cam.ac.uk/data_request/cif.

Acknowledgement

Financial support from the NNSF of China and Fujian Province are gratefully acknowledged.

[1] a) C. J. Millios, A. Vinslava, P. A. Wood, S. Parsons, W. Wernsdorfer, G. Christou, S. P. Perlepes, E. K. Brechin, *J. Am. Chem. Soc.* **2007**, *129*, 8; b) E. J. Schelter, F. Karadas, C. Avendano, A. V. Prosvirin, W. Wernsdorfer, K. M. Dunbar, *J. Am. Chem. Soc.* **2007**, *129*, 8139; c) Y.-Z. Zhang, W. Wernsdorfer, F. Pan, Z.-M. Wang, S. Gao, *Chem. Commun.* **2006**, 3302; d) T. C. Stamatatos, K. A. Abboud, W. Wernsdorfer, G. Christou, *Angew. Chem.* **2007**, *119*, 902; *Angew. Chem. Int. Ed.* **2007**, *46*, 884; e) S. Osa, T. Kido, N. Matsumoto, N. Re, A. Pochaba, J. Mrozinski, *J. Am. Chem. Soc.* **2004**, *126*, 420.

[2] a) J. R. Friedman, M. P. Sarachik, *Phys. Rev. Lett.* **1996**, *76*, 3830; b) L. Thomas, L. Lionti, R. Ballou, D. Gatteschi, R. Sessoli, B. Bar-

bara, *Nature* **1996**, *383*, 145; c) T. C. Stamatatos, D. Foguet-Albiol, S.-C. Lee, C. C. Stoumpos, C. P. Raptopoulou, A. Terzis, W. Wernsdorfer, S. O. Hill, S. P. Perlepes, G. Christou, *J. Am. Chem. Soc.* **2007**, *129*, 9484.

[3] a) W. Wernsdorfer, R. Sessoli, *Science* **2000**, *287–290,* 2417; b) W. Wernsdorfer, M. Soler, G. Christou, D. N. Hendrickson, *J. Appl. Phys.* **2002**, *91*, 7164; c) W. Wernsdorfer, N. E. Chakov, G. Christou, *Phys. Rev. Lett.* **2005**, *95*, 037203 (1–4).

[4] A. Caneschi, D. Gatteschi, N. Lalioti, C. Sangregorio, R. Sessoli, G. Venturi, A. Vindigni, A. Rettori, M. G. Pini, M. A. Novak, *Angew. Chem.* **2005**, *117*, 5967; *Angew. Chem. Int. Ed.* **2005**, *44*, 5817.

[5] a) D. Gatteschi, R. Sessoli, *Angew. Chem.* **2003**, *115*, 278; *Angew. Chem. Int. Ed.* **2003**, *42*, 268; b) A. Caneschi, D. Gatteschi, N. Lalioti, C. Sangregorio, R. Sessoli, G. Venturi, A. Vindigni, A. Rettori, M. G. Pini, M. A. Novak, *Angew. Chem.* **2003**, *115*, 278; *Angew. Chem. Int. Ed.* **2003**, *42*, 268; c) R. Lescouëzec, J. Vaissermann, C. Ruiz-Pérez, F. Loret, R. Carrasco, M. Julve, M. Verdagurer, Y. Draomzee, D. Gatteschi, W. Wernsdorfer, *Angew. Chem.* **2003**, *115*, 1521; *Angew. Chem. Int. Ed.* **2003**, *42*, 1483.

[6] a) S. Wang, J.-J. Zou, S. Gao, H.-C. Zhou, Y.-Z. Zhang, X.-Z. You *J. Am. Chem. Soc.* **2004**, *126*, 8900; b) L. Bogani, C. Sangregorio, R. Sessoli, D. Gatteschi, *Angew. Chem.* **2005**, *117*, 5967; *Angew. Chem. Int. Ed.* **2005**, *44*, 5817.

[7] a) Z.-M. Sun, A. V. Prosvirin, H.-H. Zhao, J.-G. Mao, K. R. Dunbar, *J. Appl. Phys.* **2005**, *97*, 10B305; b) J.-P. Costes, J.-M. Clemente-Juan, F. Dahan, J. Milon, *Inorg. Chem.* **2004**, *43*, 8220.

[8] L.-M. Toma, R. Lescouëzec, J. Pasan, C. Ruiz-Pérez, J. Vaissermann, J. Cano, R. Carrasco, W. Wernsdorfer, F. Lloret, M. Julve, *J. Am. Chem. Soc.* **2004**, *126*, 8900.

[9] a) Y.-L. Bai, J. Tao, W. Wernsdorfer, W. Sato, R. B. Huang, L.-S. Zheng, *J. Am. Chem. Soc.* **2006**, *128*, 16428; b) Y.-Z. Zheng, M.-L. Tong, W.-X. Zhang, X.-M. Chen, *Angew. Chem.* **2006**, *118*, 6458; *Angew. Chem. Int. Ed.* **2006**, *45*, 6310; c) T.-F. Liu, D. Fu, S. Gao, Y.-Z. Zhang, H.-L. Sun, G. Su, Y.-J. Liu, *J. Am. Chem. Soc.* **2003**, *125*, 13976.

[10] a) K. Bernot, L. Bogani, A. Caneschi, D. Gatteschi, R. Sessoli, *J. Am. Chem. Soc.* **2006**, *128*, 7947; b) L. Bogani, C. Sangregorio, R. Sessoli, D. Gatteschi, *Angew. Chem.* **2005**, *117*, 5967; *Angew. Chem. Int. Ed.* **2005**, *44*, 5817.

[11] H.-B. Xu, B.-W. Wang, F. Pan, Z.-M. Wang, S. Gao, *Angew. Chem.* **2007**, *119*, 7532; *Angew. Chem. Int. Ed.* **2007**, *46*, 7388.

[12] L. Lecren, O. Roubeau, C. Coulon, Y.-G. Li, X.-F. Le-Goff, W. Wernsdorfer, H. Miyasaka, R. Clérac, *J. Am. Chem. Soc.* **2005**, *127*, 17353.

[13] H. Miyasaka, T. Madanbashi, K. Sugimoto, Y. Nakazawa, W. Wernsdorfer, K. Sugiura, M. Yamashita, C. Coulon, R. Cléac. *Chem. Eur. J.* **2006**, *12*, 7028.

[14] H. W. Hou, G. Li, L. K. Li, Y. Zhu, X. R. Meng, Y. T. Fan, *Inorg. Chem.* **2003**, *42*, 428.

[15] a) C. Coulon, R. Cléac, L. Lecren, W. Wernsdorfer, H. Miyasaka, *Phys. Rev. B* **2004**, *69*, 132408; b) L. Bogani, A. Caneschi, M. Fedi, D. Gatteschi, M. Massi, M. A. Novak, M. G. Pini, A. Rettori, R. Sessoli, A. Vindigni, *Phys. Rev. Lett.* **2004**, *92*, 207204; c) L. Bogani, R. Sessoli, M. G. Pini, A. Rettori, M. A. Novak, P. Rosa, M. Massi, M. E. Fedi, L. Giuntini, A. Caneschi, D. Gatteschi, *Phys. Rev. B* **2005**, *72*, 064406.

[16] Y.-Z. Zheng, M.-L. Tong, W. Xue, W. X. Zhang, X. M. Chen, *Angew. Chem.* **2007**, *119*, 6188; *Angew. Chem. Int. Ed.* **2007**, *46*, 6076.

[17] a) D.-F. Li, L.-M. Zheng, Y.-Z. Zhang, J. Huang, S. Gao, W.-X. Tang, *Inorg. Chem.* **2003**, *42*, 6123; b) E. Coronado, C. J. Gómez-García, A. Nuez, F. M. Romero, J. C. Waerenborgh, *Chem. Mater.* **2006**, *18*, 2670; c) F. Pointillart, K. Bernot, R. Sessoli, D. Gatteschi, *Chem. Eur. J.* **2007**, *13*, 1602; d) B. Sarkar, M. S. Ray, Y.-Z. Li, Y. Song, A. Figuerola, E. Ruiz, J. Cirera, J. Cano, A. Ghosh, *Chem. Eur. J.* **2007**, *13*, 9297.

[18] a) S. Osa, T. Kido, N. Matsumoto, N. Re, A. Pochaba, J. Mrozinski, *J. Am. Chem. Soc.* **2004**, *126*, 420; b) H. Miyasaka, K. Nakata, L. Lecren, C. Coulon, Y. Nakazawa, T. Fujisaki, K. Sugiura, M. Yamashita, R. Cléac, *J. Am. Chem. Soc.* **2006**, *128*, 3770; c) Y.-Z. Zheng, W. Xue, W.-X. Zhang, M.-L. Tong, X.-M. Chen, *Inorg. Chem.* **2007**, *46*, 6437; d) K. S. Gavrienko, O. Cador, K. Bermpt, P. Rosa, R. Sessoli, S. Golhen, V. V. Pavilishchuk, L. Ouahab, *Chem. Eur. J.* **2008**, *14*, 2034; e) J. Tang, I. Hewitt, N. T. Madhu, G. Chastanet, W. Wernsdorfer, C. E. Anson, C. Benelli, R. Sessoli, A. K. Powell, *Angew. Chem.* **2006**, *118*, 1761; *Angew. Chem. Int. Ed.* **2006**, *45*, 1729.

Received: February 25, 2008
Revised: July 20, 2008
Published online: September 26, 2008

